



## The Effects of Subcooled Temperatures on Transient Pool Boiling of Deionized Water under Atmospheric Pressure

A. Ayoobi<sup>1</sup>, A. Faghih<sup>1\*</sup>, M. Tavakoli<sup>2</sup>

<sup>1</sup> Department of Mechanical Engineering, Yazd University, Yazd, Iran

<sup>2</sup> Department of Mechanical Engineering, Isfahan University of Technology, Isfahan, Iran

**ABSTRACT:** Pool boiling heat transfer and critical heat flux (CHF) were experimentally studied in subcooled temperatures ranging from 0°C to 20°C and under transient power conditions. A chrome-aluminum-iron alloy wire was used as the heating element. The heating rate in the test section was increased linearly depending on time by applying voltage control for 1s to 1000s. The transient boiling heat transfer coefficient (TBHTC), transient wire superheat temperature, transient heat flux and transient CHF were also obtained. The results showed that in the case of all subcooled temperatures and periods, the TBHTC increased in the nucleate boiling region because of the growth, separation, motion and turbulence of the bubbles. The TBHTC also decreased in the transition from nucleate boiling to film boiling because some part of the wire covered by temporary thin vapor film. The TBHTC again increased in film boiling due to the increment of radiation heat transfer. The TBHTC decreased in the second part of the film boiling due to the heat flux and the vapor film thickness around the wire had increased. Relative to the saturation condition, the timely average of the wire superheat temperature for subcooled temperatures of 10°C and 20°C, respectively, decreased by 9.23% and 9.29% in the nucleate boiling region and in a time period of 1000s.

### Review History:

Received: 1 Nov. 2018

Revised: 4 May. 2019

Accepted: 5 May. 2019

Available Online: 15 May. 2019

### Keywords:

Transient pool boiling

Critical heat flux

Heating rate

Subcooled temperature

Transient boiling heat transfer coefficient

### 1- Introduction

A time study of the boiling phenomenon at different times shows the complexities and importance of such a phenomenon. Images of the transient boiling phenomenon captured, for example, several heat transfer regions in nucleate boiling depending on vapor generation [1]. As the surface temperature is increased, the vapor structures are changed through a sequence of initially discrete bubbles, vapor columns, vapor mushrooms, and finally vapor patches [2]. Despite the need for a rapid heat transfer, as in 0.25-0.5 seconds [3], most studies have not taken the heating rate into account and have instead investigated the steady state mode [4-6]. The investigation into the steady state of, for example, the heat transfer time was not considered during the boiling process of a liquid, and the heat flux increased regardless of time. The time factor has become especially important in the necessity of rapid heat transfer in various applications such as nuclear reactors [3, 7-9], electronic cooling equipment [10, 11], heat exchangers [12], and etc. Due to the many differences of steady state or transient conditions [13], the form of the boiling phenomenon changes depending on the different applications and transient times and should be investigated like any other test at the desired time. Despite the extensive work present on the boiling heat transfer, much is still unknown about its physical mechanisms. Numerous analytical [14, 15]

and numerical [16, 17] studies have been carried out on this subject. The transient boiling of water and other liquids [18-20] under different kinds of the heat flux function has been investigated since the 19th century. The effects of transient power (heat flux), heat flux enhancement function and subcooling on the boiling heat transfer have been studied in previous experiments [1]. Heat flux enhancement functions include exponential [7, 21-24], quadratic [25], stepwise [18, 26, 27], ramp-wise [27, 28] and square-wave pulses [29]. Most of these studies were carried out in pool boiling conditions using wire [22, 24, 30], ribbon [13] and plate-type [7] heaters. Some forced convection studies also exist for tube [27], ribbon [31] and wire [32, 33] heaters. Li et al. performed steady and transient pool boiling experiments on a horizontal cylinder in a pool of ion-exchange-distilled water at pressures of 20 kPa to 101.6 kPa [23]. Due to an exponential increase in the heating inputs, the transient CHF for subcoolings ranging from 0 to 40 K were measured in exponential periods that ranged from 20s down to 10ms at atmospheric and sub-atmospheric pressures. Park et al. used a 1.0-mm diameter horizontal cylinder immersed in various liquids to measure the CHF levels that occurred due to exponential heat inputs at varying periods [21]. Their photographic study helped them identify two main mechanisms of CHF, one of which starts at steady-state CHF upon fully developed nucleate boiling, which is due to a time lag of the hydrodynamic instability (HI), and the other, which due to the explosive process of

\*Corresponding author's email: faghih@yazd.ac.ir



heterogenous spontaneous nucleation (HSN) occurs at a certain HSN superheat in originally flooded cavities on the cylinder surface. Su et al. presented an investigation of the transient pool boiling heat transfer phenomenon in water at atmospheric pressures and under exponentially escalating heat fluxes on plate-type heaters [7]. They used exponential power escalations with periods ranging from 5 to 100ms and subcoolings of 0, 25 and 75K. They observed an onset of nucleate boiling (ONB) conditions. Their results suggested that the onset of nucleate boiling temperature and heat flux increase monotonically by decreasing the period and increasing the subcooling temperature. Kim et al. used a high-speed infrared thermometry technique called DEPICT to investigate the nucleate boiling phenomena under various surface heat flux conditions [34]. Their results for the liquid-vapor phase distribution on a boiling surface showed the formation, coalescence, and dynamic behaviors of dry spots on a boiling surface; as the surface heat flux increased, the frequency and density of the dry spots significantly increased as well. Visentini et al. investigated transient boiling in order to better understand the influence of power excursions and to characterize the phases of the rapid boiling phenomenon [35]. Using semi annulus testing, they were able to synchronize the wall temperature measurement and flow visualization to characterize and analyze the heat transfer for the different boiling regimes: nucleate boiling, CHF and film boiling. Sharma et al. conducted pool boiling experiments for sandblasted stainless steel (grade 316) plate heaters submerged in deionized (DI) water and water-based zinc-oxide nanofluid. They increased the power quadratically with time for transient heat flux conditions. [25]. Increasing the heat flux of the experiments from zero amount of heat flux to CHF in short time frames of 1, 10 and 100s increased the transient CHF for DI water to more than that of the steady state CHF, and decreasing the transient duration increased the CHF. The present study aims to thoroughly analyze the transient saturated and subcooled pool boiling results such as temperature, heat flux, Transient Boiling Heat Transfer Coefficient (TBHTC) and CHF at atmospheric pressure and at three subcooled temperatures of 0 °C, 10 °C and 20 °C. The surface heater is a chrome-aluminum-iron alloy wire immersed in a DI water that was heated by increasing the electrical current. The input voltage was linearly increased over a period of time and heat flux generated in the heater changed approximately as the second-order polynomial function of time. Transient periods range from long times such as 1000 s (quasi-steadily) to shorter time periods such as 1 s (rapid boiling). While many other studies have investigated the effects of boiling characteristics on shorter periods. Also, their heat flux functions were exponential, step wise and ramp wise while this paper focuses on time periods greater than 1 s and second order polynomial function. This research is also among the few studies in which the boiling process is initiated by the first regime (free convection) and is continued until the final boiling regime (film boiling).

## 2- Experimental Facilities and Procedure

All components required for the experiments are shown in Fig. 1. A cylindrical pyrex vessel of 150 mm in diameter and 250 mm in height is used as the boiling vessel. The vessel was selected as the boiling cell. A hot plate with a temperature controller is used to keep the working fluid temperature

at saturation condition and subcooled conditions. The temperature of the bulk of water remains constant with the use of thermocouple and hot plate all the times at 0 °C, 10 °C and 20 °C, but the temperature of the water that is very close to the wire surface increases with increasing the heat flux and subcooled boiling was started. A plexiglass circle is used to prevent outer disturbances from entering the vessel and keep copper electrodes in position. A condenser cooled by a refrigerated circulating bath and placed on top of the vessel is used to return evaporated water to the vessel. The water level is kept constant during the boiling process. Two copper electrodes of 12 mm in diameter and 300 mm in height are used to keep the wire in position and guide the electrical current to the heater wire. This electrode is covered by shrink wrap to prevent oxidized and copper oxide from entering the DI water during the boiling process. A chrome-aluminum-iron wire of 0.15 mm in diameter and 65 mm in length is used as heater. Chrome-aluminum-iron alloy wire is firmly placed into two copper electrodes by two stainless steel washers. Before testing, the resistance-temperature coefficient is obtained through separate experiments, in which an LCR meter is used to measure the resistance and the hot plate to the rising engine oil temperature. For this purpose, the engine oil temperature is gradually increased by the hot plate, and the wire resistance is then measured at engine oil temperature. The temperature and resistance data is then moved from 20 °C to 140 °C, and the relationship between them is obtained [1]. Joule heating was used to design and build the electrical power and control circuits for this research. A power electrical circuit is required to provide the amount of power demanded by the control electrical circuit and the ability to choose the power and time periods in the tests. A direct current power supply (GPC-3060D, Gwinstek co., Ltd) is used to increase the linear input power to the wire. A precision standard shunt of 40m Ω is used to measure the current. An amplifier circuit is designed and built to put the electric current signal in the range of the High-speed Data Acquisition System (HDAS) [1]. In order to supply the amplifier circuit with ±15 V, two power supplies (Hy3020, Huayi electric co., Ltd) are considered. The instantaneous current passing through the wire heater ( $I$ ) and the associated potential drop across the wire heated length ( $\Delta V$ ) are jointly measured for each experiment and then used to calculate the wire heater temperature denoted by  $T_w(t)$  (see Eq. (2)) [1]. In order to smoothen the data and reduce the noise associated with the extremely fast data measurement, potential drop data were used to fit the desired function in the MATLAB software,  $\overline{\Delta V}$  and the current data was averaged over fixed time periods,  $\overline{I}$ :

$$\overline{R} = \frac{\overline{\Delta V}}{\overline{I}} \quad (1)$$

$$\overline{T}_w(t) = \frac{\overline{R}(t) - R_0}{\alpha R_0} + T_0 \quad (2)$$

where  $\alpha$  is the resistance-temperature coefficient for the

chrome-aluminum-iron alloy wire measured at 0.000686 / °C. The immediate heat flux is varied in time as the voltage delivered by the power circuit varies linearly with time, going from 0 to 50 V in  $t_0$  seconds, with  $t_0$  characterizing the rate of the heat flux increase. Thus, the voltage through the heater changed into  $V = 50t / t_0$ , and the power generated in the heater is changed into (approximately) the second-order polynomial function of time. Six values of  $t_0$  (time frame of linear voltage ramp from 0 to 50 V) were explored in this paper:  $t_0 = 1, 10, 100$  and  $1000$  s. Since the transient tests lasted for a short amount of time, they required high data acquisition rates. For this purpose, the voltage and current of the heater is read and saved on a personal computer by an Advantech PCI-1716 card with 250 kHz and 16-bit accuracy. Data was recorded every 2.8 milliseconds using the Advantech PCI-1716. A different steady state method is used to determine the heat flux (for that time period) transferred to the fluid. The total power is obtained by  $\bar{I}\Delta V$ ; a part of it is dissipated in the heater by the Joule effect and the rest of it transmitted to the surrounding fluid. The energy was stored in the wire at a rate of  $\rho_w c_{pw} \frac{dT_w}{dt}$ . The rate of change  $\bar{T}_w$  was approximated by the finite difference of  $0^\circ\text{C}$ ; where  $\Delta \bar{T}_w$  is the difference between two consecutive values of  $T_w$  wire, and  $\Delta t$  is the time difference between these measurements [1]. The immediate heat flux to the fluid is then calculated by

$$q'' = \frac{v}{A_w} \left( \frac{\bar{I} \Delta V}{v} - \rho_w c_{pw} \frac{dT_w}{dt} \right) \quad (3)$$

The TBHTC value can be calculated from the heat flux and the wire superheat temperature ( $\Delta T_w = \bar{T}_w - T_0$ ) through the following equation:

$$h = \frac{q''}{\Delta T_w} \quad (4)$$

The method proposed by Moffat [36] is used for the uncertainty analysis. The voltage accuracy of data card at the  $\pm 10\text{V}$  range is 0.05 V. The measured ripple of the input signal by oscilloscope was less than 5 mV. The shunt accuracy is 0.1% and the temperature coefficient of shunt is 0.02% which were considered to calculate the current uncertainty. Colis instrument was used to measure the wire length and diameter that its accuracy is 0.02 mm. The number of samples is  $N$ , the mean value of quantity  $x$  is defined by Eq. (5) and the corresponding type  $x$  uncertainty in terms of expected value  $\sigma(x)$  and the standard uncertainty  $U(x)$  associated with it can be evaluated by Eqs. (6) and (7) respectively. The relative uncertainty for wire area, wire temperature, current and heat flux can be reached by Eqs. (9) to (12) respectively:

$$E(x) = \frac{1}{N} \sum_{i=1}^N x_i \quad (5)$$

$$\sigma(x) = \sqrt{\frac{\sum_{i=1}^N [x_i - E(x)]^2}{N-1}} \quad (6)$$

$$U(x) = \frac{\sigma(x)}{\sqrt{N}} \quad (7)$$

$$\bar{I} = \frac{\Delta V}{R_{shunt}} \quad (8)$$

$$\frac{U_A}{A} = \left[ \left( \frac{U_r}{r} \right)^2 + \left( \frac{U_l}{l} \right)^2 \right]^{0.5} \quad (9)$$

$$\frac{U_{T_w}}{T_w} = \left[ \left( \frac{U_{\Delta V}}{\Delta V} \right)^2 + \left( \frac{U_{\bar{I}}}{\bar{I}} \right)^2 \right]^{0.5} \quad (10)$$

$$\frac{U_{\bar{I}}}{\bar{I}} = \left[ \left( \frac{U_{\Delta V}}{\Delta V} \right)^2 + \left( \frac{U_{R_{shunt}}}{R_{shunt}} \right)^2 \right]^{0.5} \quad (11)$$

$$\frac{U_{q''}}{q''} = \left[ \left( \frac{U_{\Delta V}}{\Delta V} \right)^2 + \left( \frac{U_{\bar{I}}}{\bar{I}} \right)^2 + \left( \frac{U_A}{A} \right)^2 + \left( \frac{U_r}{r} \right)^2 + \left( \frac{U_{T_w}}{T_w} \right)^2 + \left( \frac{U_t}{t} \right)^2 \right]^{0.5} \quad (12)$$

The uncertainties in potential drop, the current and area of the wire are calculated to be approximately 0.35%, 0.57% and 2.3%, respectively. The uncertainties of the estimated wire temperature and heat flux to the fluid are roughly 0.17% and 2.31%.

### 3- Results and Discussion

#### 3- 1- Validation and repeatability

The experimental results are compared with the Rohsenow [37] and Zuber [38] correlations for the steady state boiling of DI water shown in Fig. 2. The experimental results in the nucleate boiling are in good agreement and closely follow the Rohsenow correlation. Also, the obtained CHF amount is close to the predicted value of the Zuber correlation [1]. The Rohsenow and Zuber correlations are used to validate

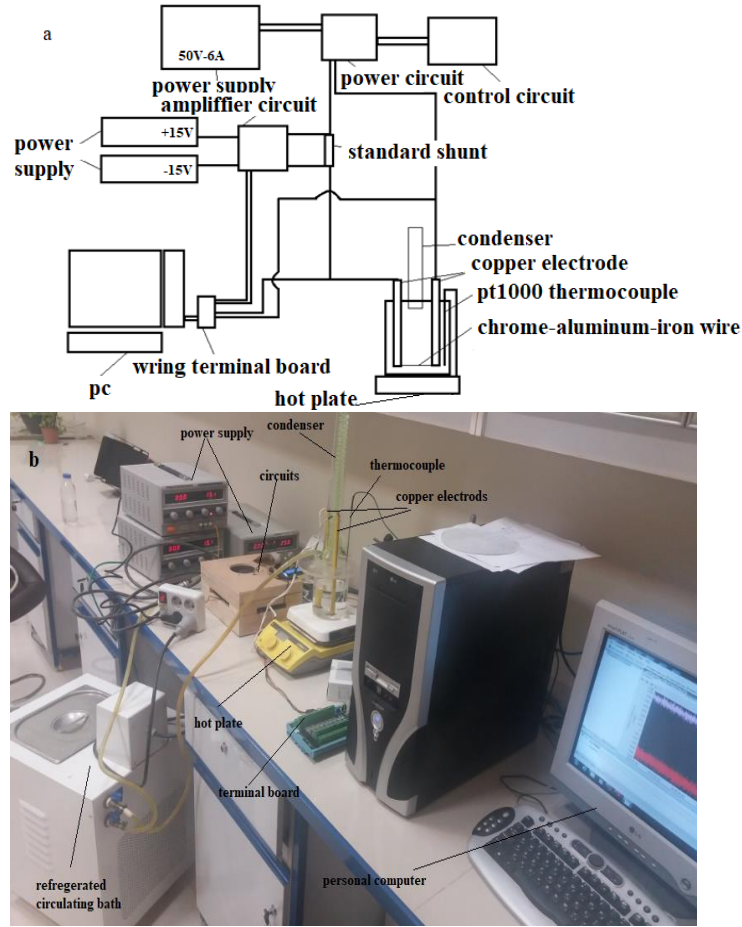


Fig. 1. Schematic of experimental facilities, a) schematic view, b) actual image .

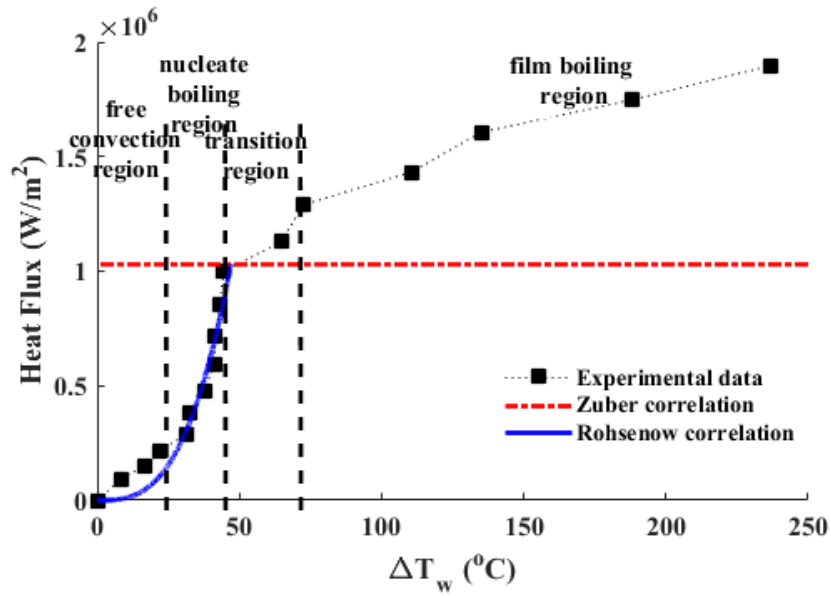


Fig. 2. Experimental results of DI boiling water compared with Rohsenow correlation [1].

the nucleate boiling region and CHF value in the empirical works, as expressed in the following equations:

$$\Delta T_s = \frac{h_{fg}}{C_{p,l}} C_{sf} \left[ \frac{q''}{\mu_l h_{fg}} \left( \frac{\sigma}{g(\rho_l - \rho_v)} \right)^{0.5} \right]^{\frac{1}{3}} Pr^n \quad (13)$$

$$q''_{CHF} = 0.131 h_{fg} \rho_v^{0.5} (g \sigma (\rho_l - \rho_v))^{1/4} \quad (14)$$

After nucleate boiling, the power continued to increase during the transition from nucleate boiling to film boiling and film boiling, respectively. In the steady state test, the power increase is incremental, and for each step, the voltage value is increased by one volt. As shown in the figure, following the CHF, the wire superheat temperature of each data increased considerably compared to that of the nucleate boiling and free convection region. All of the steps for increasing the power were, however, equal [1]. Fig. 3 shows the transient boiling curve for a period of 1 s [1]. The free convection regime is extended to point A to an abnormally more than steady state, and the nucleate boiling regime is delayed. According to Htet et al. [39], increasing the heat exponentially causes a stretch in the free convection regime. The nucleate boiling point is started after point A. In fact, the wire temperature rises once boiling initiates explosively with nucleate boiling, which is simultaneously followed by a rapid increase of the heat input. Nucleate boiling is then continued to point B. At this point, the boiling curve route is changed, causing an abrupt increase in the wire temperature and sending the pool boiling into the next regime. The transition from nucleate boiling to film boiling is conducted in a short time, largely effecting on the pool boiling and heat transfer mechanism (wire temperature and heat flux from point B to point C). During the transition from nucleate boiling to film boiling, the vapor

film was formed temporarily around portions of the wire and disappeared, momentarily increasing and decreasing the wire temperature, bubble departure rate and bubble figure.

Film boiling is started permanently at point C as a very thin and stable vapor film around the wire. The wire temperature in the film boiling regime is increased by increasing the heat flux and preventing any contact with water. The wire is easily visible as a glowing red color. As heating continues, the heat flux and wire temperature in the film boiling are increased, and the high wire temperature is seen in glowing red wire. The slope of the film boiling is lowered at point D, and the wire temperature is greatly increased by the heat flux from thereon, which is due to an increase in the thickness of the vapor film around the wire. The high wire temperature allows the larger vapor film to retain its thickness around the wire. Also, increasing the thickness of the vapor film decreases the amount of heat transfer from the wire to water, and as a result, the temperature of the wire is increased further than the range between points C and D. As suggested by Sakurai and Fukuda [40], semi-direct transition would be assumed to occur from non-boiling regime to last regime (film boiling) because of the instantaneous levitation of the working fluid from the wire surface by the explosive-like HSN. The HSN occurs easily at 0 °C [1].

### 3- 2- Comparing subcooled DI water conditions

Fig. 4 shows the transient pool boiling for periods of 1 and 1000 s. The heat flux, wire superheat temperature and TBHTC are shown at three different subcooled temperatures of 0, 10 and 20 °C in two groups. These parameters are expressed in a time period of 1 s in the first group (left hand), and a time period of 1000 s in the second group (right hand). To properly display the parameters together, the wire superheat temperature is multiplied by 100 and 1000 factors for time periods of 1 and 1000 s, respectively. In both groups, the final heat flux and the TBHTC are increased, which also increased the subcooled DI water because of the higher level of liquid subcooling temperature, higher heat flux and TBHTC. The higher subcooling temperature needs more heat flux to initiate and sustain bubble activity. When the bubbles grow, they contact the subcooled bulk working fluid at the liquid-vapor interface that causing condensation. The behavior of the wire superheat temperature depends on the characteristics of the wire material, the heat increase rate and the heat transfer mechanism from the wire to the surrounding environment. As shown in Fig. 4, the wire superheat temperature curve is changed drastically by increasing the degree of the subcooled water. In saturation conditions, heat transfer mechanisms are observed from free convection to film boiling, but at other subcooled water degrees, the transition from the nucleate boiling to film boiling regime and the film boiling regime are gradually removed. This occurrence can be explained that more heat flux is required for each boiling regime by increasing the subcooled temperature of the working fluid. This causes increasing the amount of heat flux in the regimes before the transition regime or film boiling regimes. Therefore, more nucleation sites are activated. On the other hand, the thickness of superheated layer around the wire decreased by increasing subcooled temperature. As a results, the bubble growth and separation rate decreased because of condensation. This causes that the heat generated is not completely transmitted. So, the wire superheat temperature

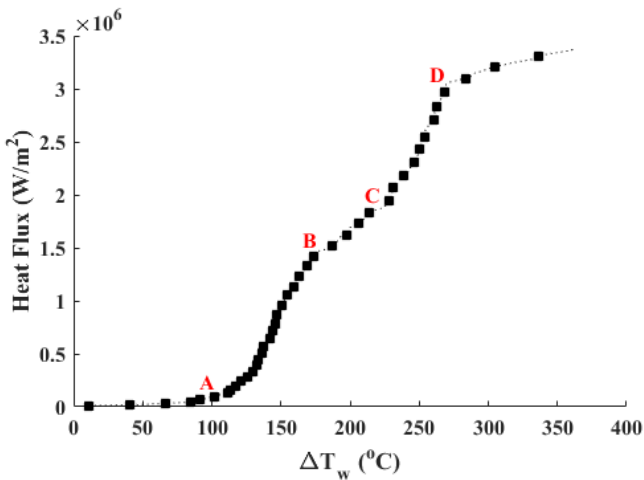


Fig. 3. Transient boiling curve for period of 1 s [1].

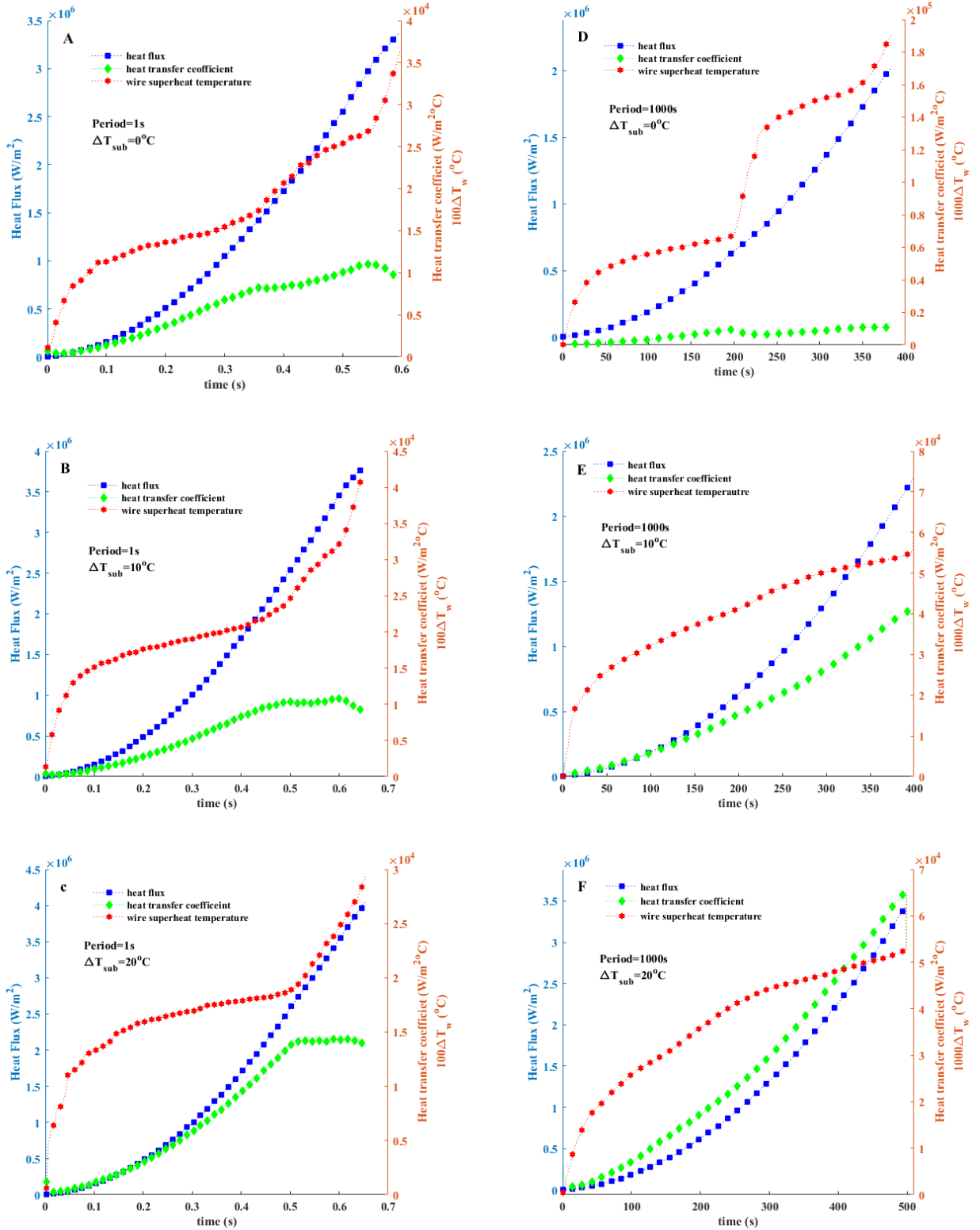


Fig. 4. Experimental results of transient boiling for time period 1 s and 1000 s A,D)  $0^\circ C$ , B,E)  $10^\circ C$ , C,F)  $20^\circ C$ .

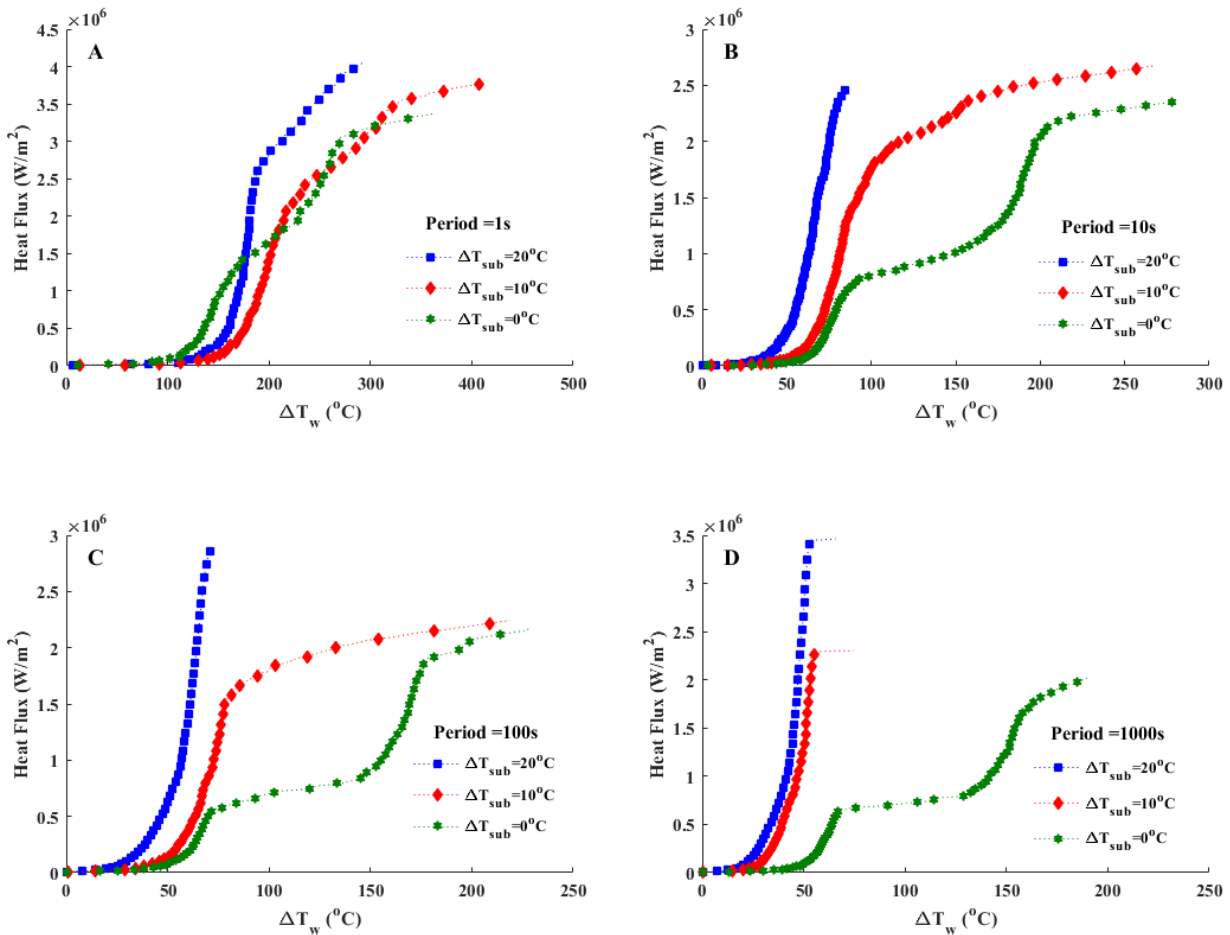


Fig. 5. Transient pool boiling curve for the time period of A)1 s, B)10 s, C)100 s and D)1000 s.

suddenly increases and the wire melts at one point. The boiling process time for the subcooled temperatures of 10 °C and 20 °C is increased by 7% and 9% in a time period of 1s and 4% and 30.2% in a period of 1000 s relative to the saturation condition, respectively. Therefore, in a constant period, duration of the boiling process from free convection to film boiling increases as the subcooled degree is increased. Timely averaged heat flux at subcooled temperatures of 10 °C and 20 °C increased by 11.5% and 16.7% for a period of 1s, and 10.1% and 64.3% for a period of 1000 s relative to the saturation condition, respectively. The test time and heat flux in each group are increased as the subcooled degree increases and the wire superheat temperature decreases (except for a period of 1s and a subcooled degree of 10 °C). The typical pool boiling charts for the four periods at three degrees of subcooled water are shown in Figs. 5 and 6, respectively. Fig. 5 illustrates that the wire superheat temperature at subcooled temperatures of 10 °C and 20 °C in a period of 1s is more than the wire superheat temperature at saturation conditions of the same heat flux. This is related to the bubble behavior and the insufficient enhancement of the boiling heat transfer coefficient. The less thickness of superheat layer prevents from the bubble growth and separation from wire. Hence,

the bubble separation frequency and bubble separation size decreased. As a result, the TBHTC decreased and wire superheat temperature increased. Thus, activation of new nucleation sites on the wire is expected to occur much faster for high subcooled water during short periods than for low subcooled water during long periods. In the long periods, the wire superheat temperature is decreased as the subcooled temperature increases.

The timely average of the wire superheat temperature in the nucleate boiling regime in a time period of 1000 s is decreased by 9.23% and 9.29% relative to the saturation condition, respectively, at 10 °C and 20 °C. Furthermore, at any given time period expect at time period 1s, the nucleate boiling regime starts earlier if the subcooling of water is increased (this trend was seen by Su et al. [7] in the exponential escalation of heat inputs). This is because of the rates of heat transfer and temperature rise of liquid layer close to the wire during heating to end of the free convection regime. This causes that the superheat layer was formed. So, the huge number of cavities that entrained vapor are rapidly activated and produces tiny vapor bubbles. The transient pool boiling results for each subcooled temperature is seen in Fig. 6. A comparison of the subcooled temperatures shows that nucleate

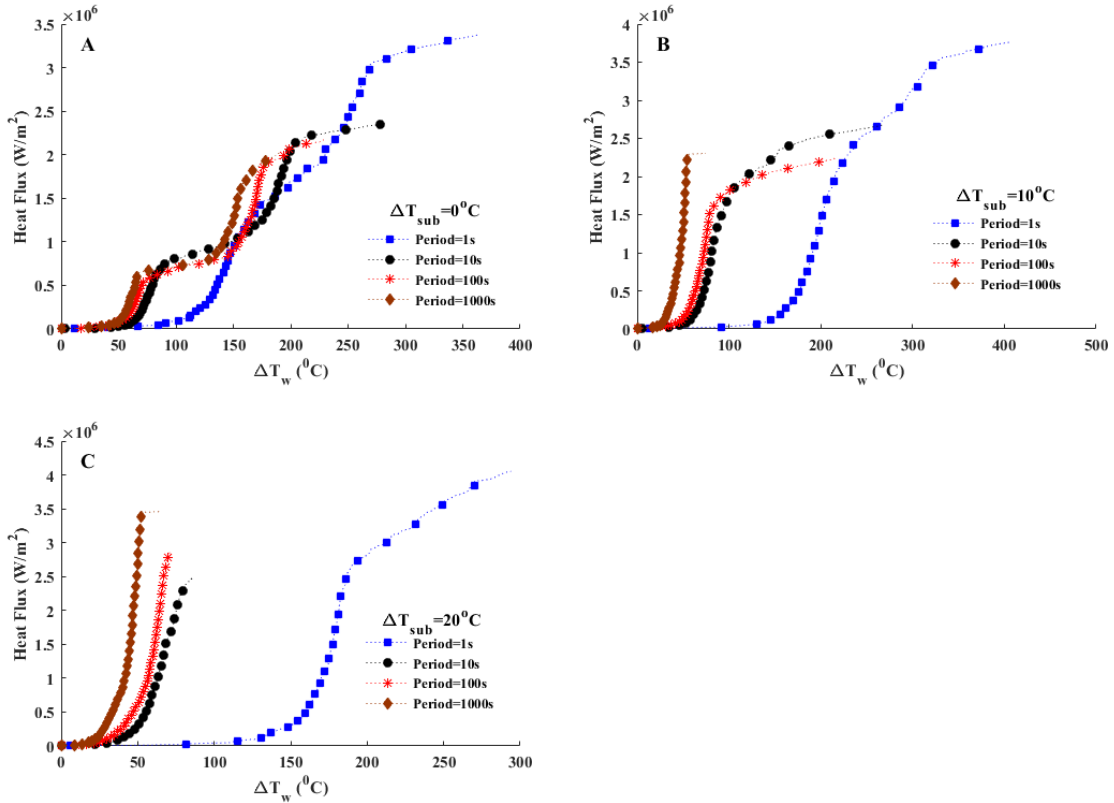


Fig. 6. Comparison of transient pool boiling curve for subcooled degrees of A) 0°C, B) 10°C and C) 20°C .

boiling decreased initially and then increased. Furthermore, the results of this figure indicate that the temperature of the wire superheat is at its highest in a 1s period and then begins to decrease. It's because of getting away from the HSN and increasing the bubble separation frequency. The nucleate boiling region in saturation conditions, 10°C and 20°C degrees of subcooled temperature, is not reduced any further at the time periods of 100 s, 100 s, and 10 s, respectively, and is, rather, increased thereafter. This is the result of two simultaneously effect of the long time period and subcooled temperatures of working fluid, which increase the number of nucleate sites and increase the thickness of superheated layer.

Fig. 7 shows the TBHTC vs. heat flux for periods of 1, 10, 100 and 1000 s, in addition to the subcooled temperatures of 0°C, 10°C and 20°C degrees. As shown in Fig. 7, except for the 1s period, the TBHTC is higher at the subcooled temperature of 20°C than at the other subcooled temperatures, and the TBHTC increases with increasing the subcooled temperatures from 0°C to 20°C because of the lower body temperature of the working fluid than saturation condition.

The TBHTC of the saturation condition in a 1s period at the heat flux of 1.45 MW/m<sup>2</sup> is more than the other periods. The increase in the TBHTC in the nucleate boiling regime in a 1s period for the subcooled temperatures of 10°C and 20°C is 28.7% and 53.9% relative to the saturation condition, respectively.

Fig. 8 illustrates the results of the CHF for four time periods and three subcooled temperatures of water. As can be seen, increasing the subcooled temperature of the working fluid

increases the CHF. The amount of heat flux produced in the nucleate boiling regime increased by increasing of working fluid subcooled temperature, resulting in a higher heat flux at the end of the nucleate boiling. The CHF of the subcooled temperatures of 10°C and 20°C for a 1s period is increased by 68.1% and 86.5% relative to the saturation condition; while this increase for a period of 1000s was 257.7% and 436.7%, respectively.

During the increasing period, the CHF decreased and reached a minimum initially and then increased. It was because of the semi-direct transition would occur from the free convection region to the film boiling due to the instantaneous levitation of the working fluid from the wire surface by the explosive-like HSN. Furthermore, with an increase in the subcooled temperature, the minimum CHF occurred in a shorter period of time. The wire superheat temperature at the CHF is decreased as the time periods for all subcooled temperature are increased.

#### 4- Conclusion

Pool boiling heat transfer and CHF in subcooled temperatures of 0°C, 10°C and 20°C were experimentally studied under transient power conditions. A chrome-aluminum-iron alloy wire supported horizontally in a pool of water was used as the heating element. The heating rate in the test section was increased linearly depending on the time periods by applying voltage control for 1 s to 1000 s. The heat flux is obtained by a second-order function of time. The experimental results in nucleate boiling are in good

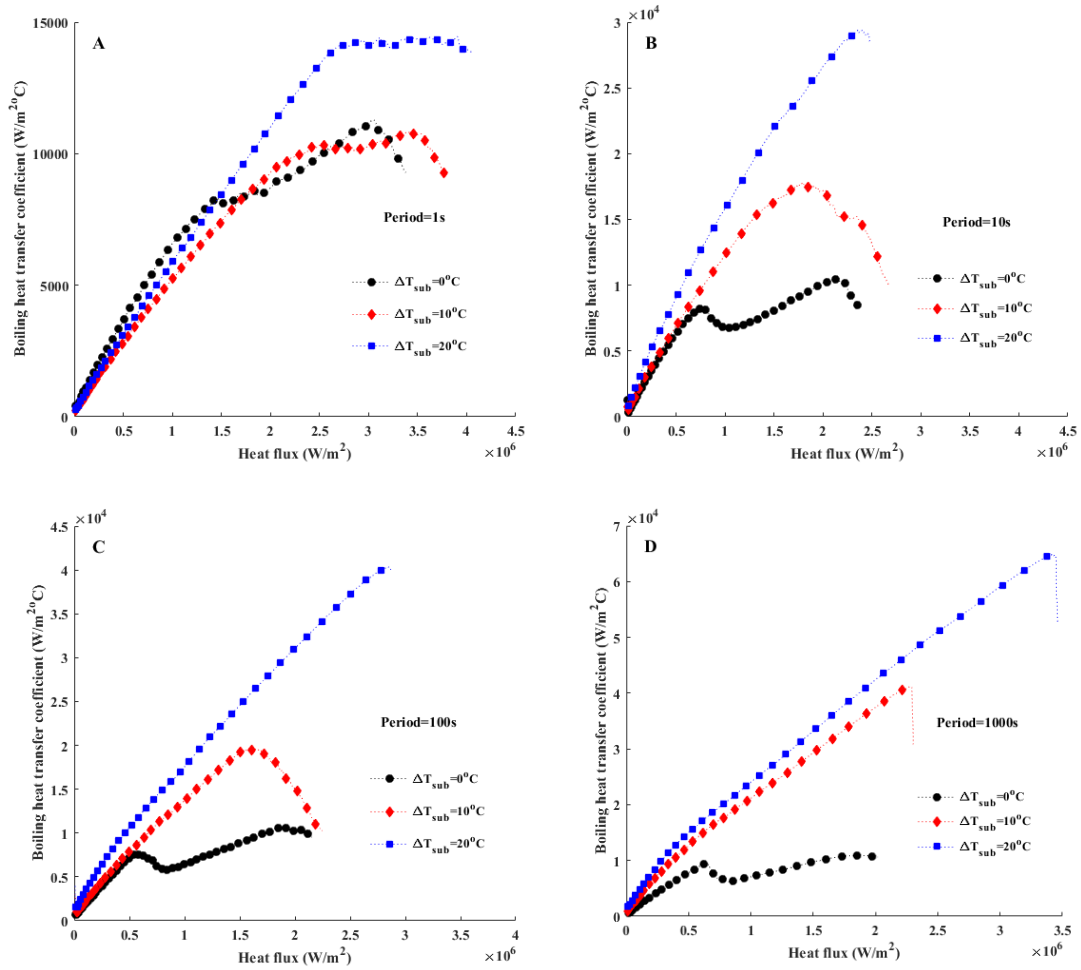


Fig. 7. TBHTC vs. heat flux for the time periods of A)1s, B)10s, C)100s and D)1000s.

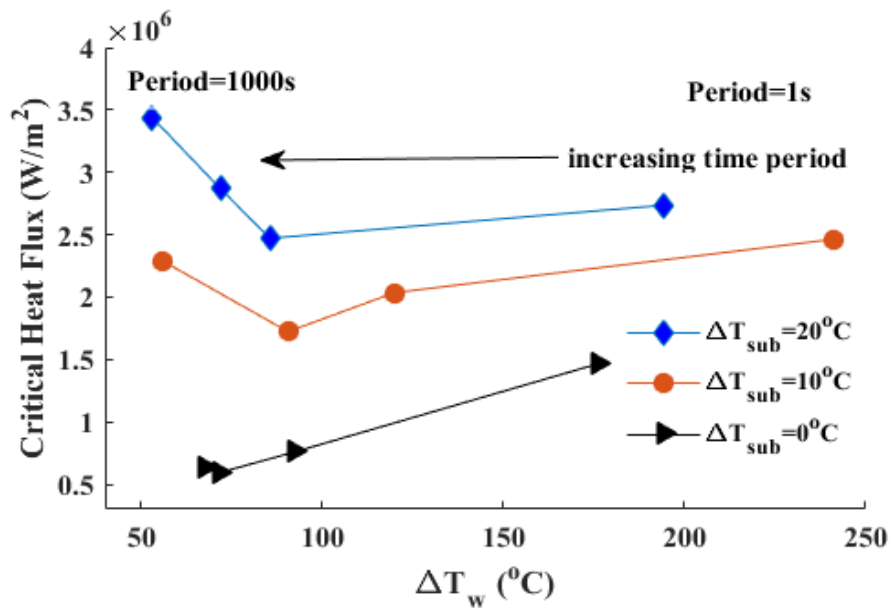


Fig.8. Transient CHF results for subcooled conditions of 0°C , 10°C and 20°C .

agreement and closely follow the Rohsenow correlation. Also, the CHF is in proximity to the predicted value of the Zuber correlation. Results showed that the behavior of the wire superheat temperature depends on the characteristics of the wire material, the rate of the heat increase and the heat transfer mechanism from the wire to the surrounding environment. The nucleate boiling regime in the 1s period and under the subcooled temperatures of 10°C and 20°C had a TBHTC increase of 28.7% and 53.9% relative to the saturation condition, respectively. The CHF of the subcooled temperatures of 10°C and 20°C was increased by 68.1% and 86.5% in a period of 1 s, while the increase in a period of 1000 s was 257.7% and 436.7% relative to the saturation condition, respectively. The wire superheat temperature at CHF's for each of the subcooled temperatures was decreased as the time periods increased.

## Nomenclature

### Latin letters

$A_w$	Heat transfer area ( $m^2$ )
$C_{p_w}$	Specific heat capacity of the wire heater material ( $kJ/kg \cdot ^\circ C$ )
$C_{sf}$	Chrome-aluminum-iron alloy constant
$g$	Gravity acceleration ( $m/s^2$ )
$h$	Heat transfer coefficient ( $W/m^2 \cdot ^\circ C$ )
$h_{fg}$	Fluid's latent heat ( $kJ/kg$ )
$\bar{I}$	Average current (A)
$n$	Chrome-aluminum-iron alloy constant
$Pr$	Prandtl number
$q''$	Heat flux ( $W/m^2$ )
$R$	Resistance ( $\Omega$ )
$T$	Temperature ( $^\circ C$ )
$t$	Time period
$v$	Heater volume ( $m^3$ )

### Greek letters

$\alpha$	Resistance-temperature coefficient ( $1/^\circ C$ )
$\mu$	Dynamic viscosity ( $N/m^2$ )
$\rho$	Density ( $kg/m^3$ )
$\sigma$	Surface tension ( $N/m$ )
$\overline{\Delta V}$	Average potential drop (V)
$\Delta T$	Wire superheat temperature ( $= \bar{T}_w - T_0$ ) ( $^\circ C$ )

$$\Delta T_{sub} = T_0 - T_{subcooled\ water}$$

### Subscripts

0	Saturation condition
CHF	Critical heat flux
l	Liquid
sub	Subcooled
v	Vapor
w	Wire

### Superscripts

-	Average
---	---------

## References

- [1] A. Ayoobi, A.F. Khorasani, M.R. Tavakoli, M.R. Salimpour, Experimental study of the time period of continued heating rate on the pool boiling characteristics of saturated water, *International Journal of Heat and Mass Transfer*, 137 (2019) 318-327.
- [2] R.F. Gaertner, Photographic study of nucleate pool boiling on a horizontal surface, *Journal of Heat Transfer*, 87(1) (1965) 17-27.
- [3] H. Finnemann, O.f.E. Co-operation, Development, Results of LWR core transient benchmarks, in: Organization for Economic Co-operation and Development, 1993.
- [4] A. Zou, A. Chanana, A. Agrawal, P.C. Wayner Jr, S.C. Maroo, Steady state vapor bubble in pool boiling, *Scientific reports*, 6 (2016).
- [5] S. Jun, J. Kim, S.M. You, H.Y. Kim, Effect of heater orientation on pool boiling heat transfer from sintered copper microporous coating in saturated water, *International Journal of Heat and Mass Transfer*, 103 (2016) 277-284.
- [6] J. Wang, F.-C. Li, X.-B. Li, Bubble explosion in pool boiling around a heated wire in surfactant solution, *International Journal of Heat and Mass Transfer*, 99 (2016) 569-575.
- [7] G.-Y. Su, M. Bucci, T. McKrell, J. Buongiorno, Transient boiling of water under exponentially escalating heat inputs. Part I: Pool boiling, *International Journal of Heat and Mass Transfer*, 96 (2016) 667-684.
- [8] S.D. Park, S.W. Lee, S. Kang, S.M. Kim, I.C. Bang, Pool boiling CHF enhancement by graphene-oxide nanofluid under nuclear coolant chemical environments, *Nuclear Engineering and Design*, 252 (2012) 184-191.
- [9] M. Hursin, T. Downar, PWR control rod ejection analysis with the MOC code decart, in: Joint International Workshop: Nuclear Technology Society—Needs for Next Generation, Berkley, CA, 2008.
- [10] M.S. El-Genk, Immersion cooling nucleate boiling of high power computer chips, *Energy Conversion and Management*, 53(1) (2012) 205-218.
- [11] A.F. Ali, M.S. El-Genk, Spreaders for immersion nucleate boiling cooling of a computer chip with a central hot spot, *Energy Conversion and Management*, 53(1) (2012) 259-267.
- [12] Y. Zhang, D. Lu, Z. Wang, X. Fu, Q. Cao, Y. Yang, Experimental investigation on pool-boiling of C-shape heat exchanger bundle used in PRHR HX, *Applied Thermal Engineering*, 114 (2017) 186-195.
- [13] M.W. Rosenthal, An experimental study of transient boiling, *Nuclear Science and Engineering*, 2(5) (1957) 640-656.
- [14] K. Pasamehmetoglu, R. Nelson, F. Gunnerson, Critical heat flux modeling in pool boiling for steady-state and power transients, *Journal of Heat Transfer*, 112(4) (1990) 1048-1057.
- [15] M. Danish, M.K. Al Mesfer, Analytical solution of nucleate pool boiling heat transfer model based on macrolayer, *Heat and Mass Transfer*, (2017) 1-12.
- [16] V.K. Dhir, G.R. Warrier, E. Aktinol, Numerical

- simulation of pool boiling: a review, *Journal of Heat Transfer*, 135(6) (2013) 061502.
- [17] C. Marcel, A. Clause, C. Frankiewicz, A. Betz, D. Attinger, Numerical investigation into the effect of surface wettability in pool boiling heat transfer with a stochastic-automata model, *International Journal of Heat and Mass Transfer*, 111 (2017) 657-665.
- [18] J.S. Ervin, H. Merte, R. Keller, K. Kirk, Transient pool boiling in microgravity, *International journal of heat and mass transfer*, 35(3) (1992) 659-674.
- [19] A. Pavlenko, E. Tairov, V. Zhukov, A. Levin, A. Tsoi, Investigation of transient processes at liquid boiling under nonstationary heat generation conditions, *Journal of Engineering Thermophysics*, 20(4) (2011) 380-406.
- [20] H. Auracher, W. Marquardt, Experimental studies of boiling mechanisms in all boiling regimes under steady-state and transient conditions, *International Journal of Thermal Sciences*, 41(7) (2002) 586-598.
- [21] J. Park, K. Fukuda, Q. Liu, Critical heat flux phenomena depending on pre-pressurization in transient heat input, in: *AIP Conference Proceedings*, AIP Publishing, 2017, pp. 080005.
- [22] M. Shiotsu, Transient Pool Boiling Heat Transfer, *Journal of Heat Transfer*, 99 (1977) 547.
- [23] Y. LI, K. FUKUDA, Q. LIU, Steady and Transient CHF in Subcooled Pool Boiling of Water under Sub-atmospheric Pressures, *Marine engineering: journal of the Japan Institute of Marine Engineering*, 52(2) (2017) 245-250.
- [24] A. Sakurai, M. Shiotsu, Transient Pool Boiling Heat Transfer—Part 2: Boiling Heat Transfer and Burnout, *Journal of heat transfer*, 99(4) (1977) 554-560.
- [25] V.I. Sharma, J. Buongiorno, T.J. McKrell, L.W. Hu, Experimental investigation of transient critical heat flux of water-based zinc-oxide nanofluids, *International Journal of Heat and Mass Transfer*, 61 (2013) 425-431.
- [26] S.M. Kwark, R. Kumar, G. Moreno, S.M. You, Transient characteristics of pool boiling heat transfer in nanofluids, *Journal of Heat Transfer*, 134(5) (2012) 051015.
- [27] K. Hata, S. Masuzaki, Influence of heat input waveform on transient critical heat flux of subcooled water flow boiling in a short vertical tube, *Nuclear Engineering and Design*, 240(2) (2010) 440-452.
- [28] F. Tachibana, M. Akiyama, H. Kawamura, Heat transfer and critical heat flux in transient boiling.(i) an experimental study in saturated pool boiling, *Journal of Nuclear Science and Technology*, 5(3) (1968) 117-126.
- [29] K. Derewnicki, Experimental studies of heat transfer and vapour formation in fast transient boiling, *International journal of heat and mass transfer*, 28(11) (1985) 2085-2092.
- [30] A. Sakurai, M. Shiotsu, K. Hata, K. Fukuda, Photographic study on transitions from non-boiling and nucleate boiling regime to film boiling due to increasing heat inputs in liquid nitrogen and water, *Nuclear Engineering and Design*, 200(1) (2000) 39-54.
- [31] H. Johnson, Transient boiling heat transfer to water, *International Journal of Heat and Mass Transfer*, 14(1) (1971) 67-82.
- [32] K. Isao, S. Akimi, S. Akira, Transient boiling heat transfer under forced convection, *International Journal of Heat and Mass Transfer*, 26(4) (1983) 583-595.
- [33] A. Sakurai, A. Serizawa, I. Kataoka, M. Shiozu, Transient boiling heat transfer under forced convection, *Kyoto Daigaku Genshi Enerugi Kenkyusho Iho*, (1978) 16-19.
- [34] D.E. Kim, J. Song, H. Kim, Simultaneous observation of dynamics and thermal evolution of irreversible dry spot at critical heat flux in pool boiling, *International Journal of Heat and Mass Transfer*, 99 (2016) 409-424.
- [35] R. Visentini, C. Colin, P. Ruyer, Experimental investigation of heat transfer in transient boiling, *Experimental Thermal and Fluid Science*, 55 (2014) 95-105.
- [36] R.J. Moffat, Describing the uncertainties in experimental results, *Experimental thermal and fluid science*, 1(1) (1988) 3-17.
- [37] W.M. Rohsenow, A method of correlating heat transfer data for surface boiling of liquids, Cambridge, Mass.: MIT Division of Industrial Cooperation, [1951], 1951.
- [38] N. Zuber, Nucleate boiling. The region of isolated bubbles and the similarity with natural convection, *International Journal of Heat and Mass Transfer*, 6(1) (1963) 53-78.
- [39] M.H. Htet, K. Fukuda, Q. Liu, Transient boiling critical heat flux on horizontal vertically oriented ribbon heater with treated surface condition in pool of water, *Mechanical Engineering Journal*, 3(3) (2016) 15-00438-00415-00438.
- [40] [40] A. Sakurai, K. Fukuda, Mechanisms of subcooled pool boiling CHF's depending on subcooling, pressure, and test heater configurations and surface conditions in liquids, in: *ASME 2002 International Mechanical Engineering Congress and Exposition*, American Society of Mechanical Engineers, 2002, pp. 213-225.

